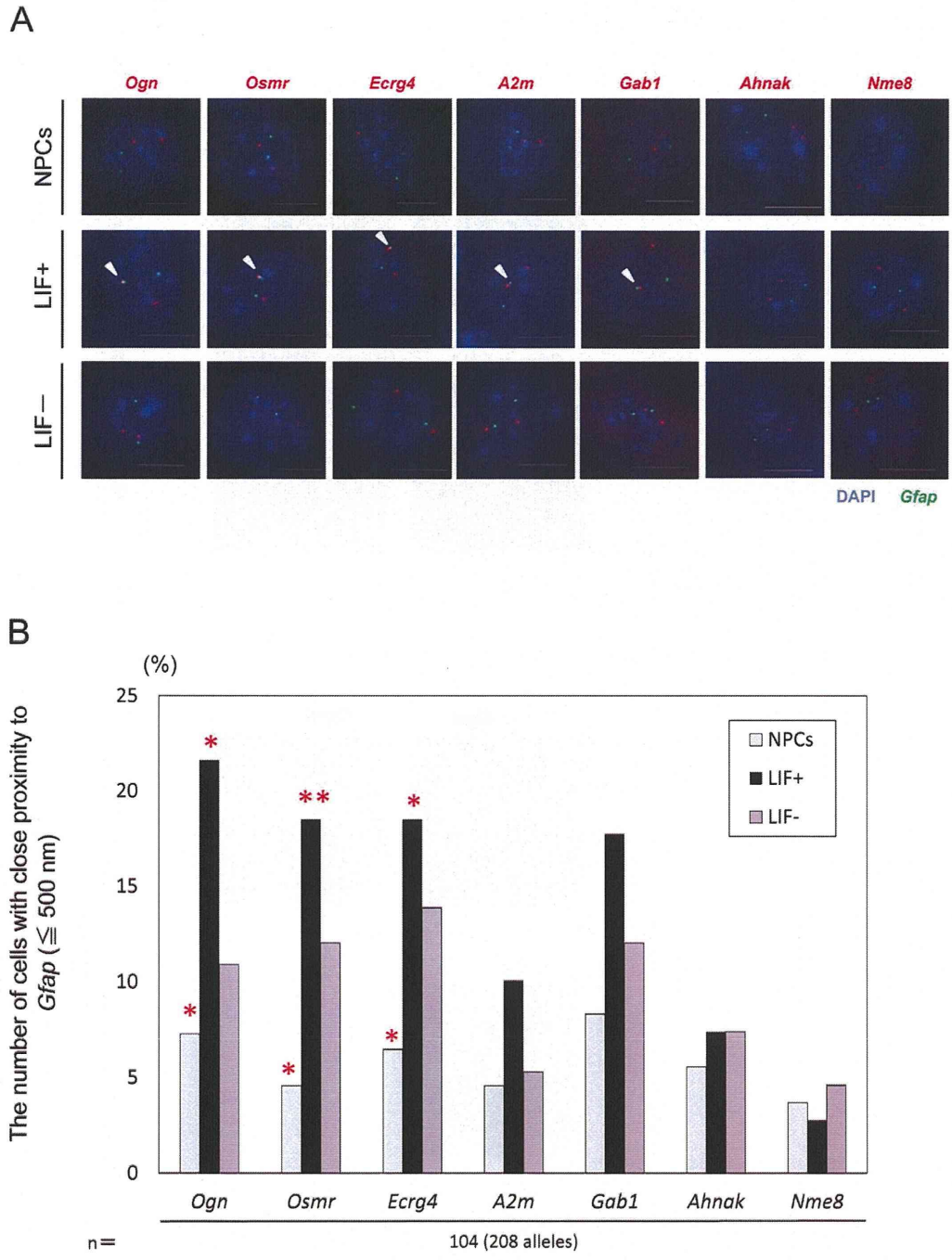

Figure 4. Validation of gene association between *Gfap* and five putative genes identified by Genechip and modified e4C. (**A**) Projected images of double-labeled DNA FISH in NPCs, LIF+, and LIF− cells for *Gfap* (green) and other genes (red). Nuclei were counterstained with DAPI (blue). Scale bar = 5 μm. (**B**) Association frequencies determined with DNA FISH for the indicated gene pairs in NPCs, LIF+, and LIF− cells. $^{**}P < 0.01$, $^{*}P < 0.05$. (**C**) Nuclear size as measured by DAPI staining in NPCs, LIF+, and LIF− cells. $^{**}P < 0.01$, $^{*}P < 0.05$.

methylation can enhance gene associations and change transcription states[47]. Thus, it would be interesting to investigate replication timing and genome-wide epigenetic modifications in NPCs and NPC-derived astrocytes. In this sense, it will also be interesting to identify genes that associate with *Gfap* in NPCs from mouse telencephalon at mid-gestation (e.g., E11.5) because the promoter region of *Gfap* is highly DNA methylated and H3K27 is tri-methylated to maintain a transcriptionally repressed state[19,48].

Recent studies that couple 3C derivatives and deep sequencing have shown that the genome's spatial organization is more complex than initially thought. Dixon *et al.*[49] showed that the genome is organized into large, discrete, and self-interacting domains and termed these "topological domains." These serve as a fundamental

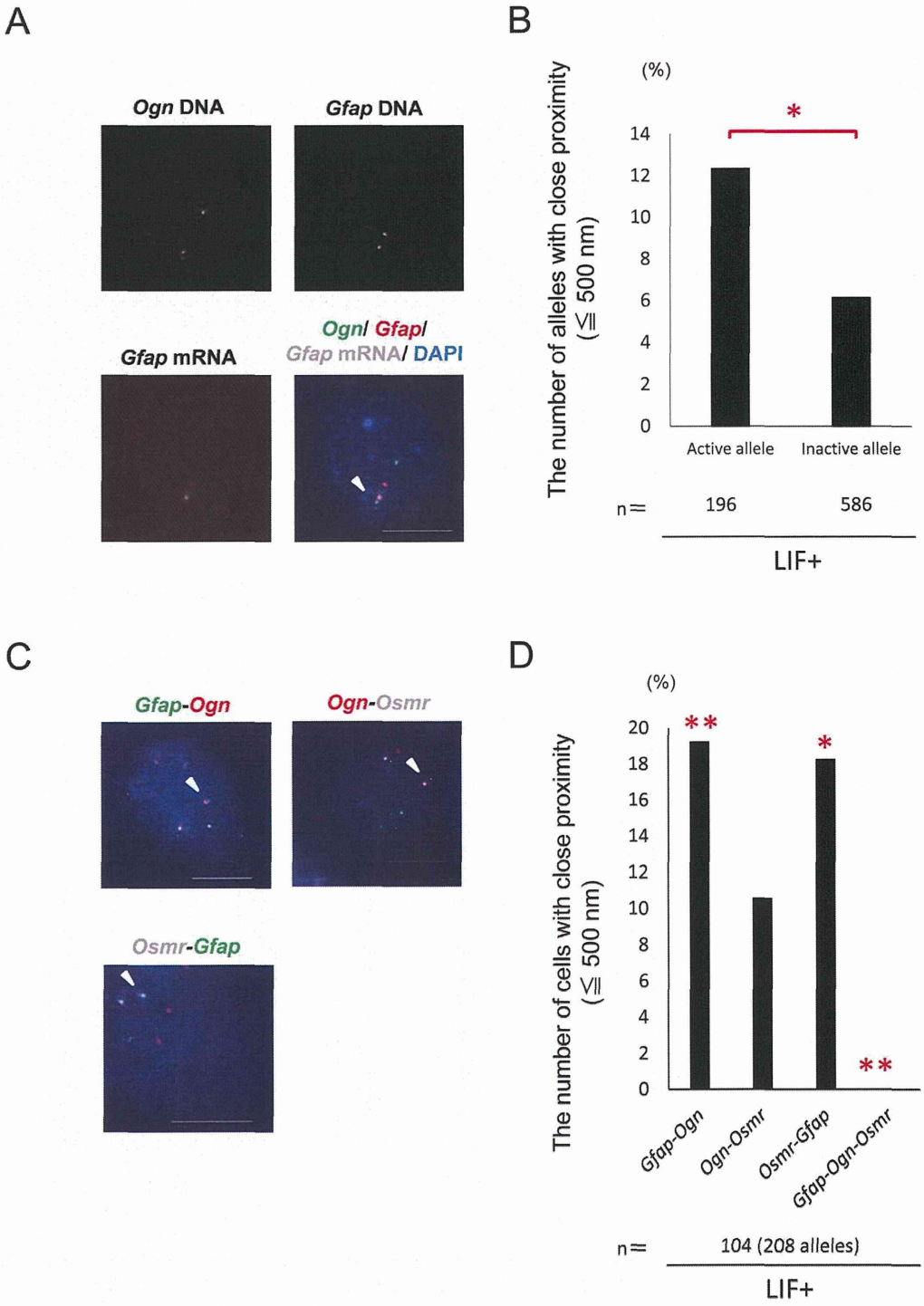

Figure 5. Detailed gene association analysis. (**A**) Projected images of triple-labeled RNA/DNA FISH in LIF+ cells for *Ogn* DNA (green), *Gfap* RNA (red), and *Gfap* DNA (white). Nuclei were counterstained with DAPI (blue). Scale bar = 5 μm. (**B**) Association frequencies of *Gfap* active alleles and inactive alleles determined with RNA/DNA FISH for LIF+ cells. *$P < 0.05$. (**C**) Projected images of triple-labeled DNA FISH in LIF+ cells for *Gfap* (green), *Ogn* (red), and *Osmr* (white). Nuclei were counterstained with DAPI (blue). Scale bar = 5 μm. (**D**) Association frequencies determined with DNA FISH for the indicated gene pairs in LIF+ cells. **$P < 0.01$, *$P < 0.05$.

organizational framework of the genome because the broader organization of these topological domains is largely unchanged during differentiation, and structural changes mostly occur within domains[49,50]. In this study, we found both specifically associating genes and genes that stably associate with *Gfap*. Although their molecular functions and significances remain unknown, they presumably act as the boundaries of topological domain-like structures and may play a role in cell-type-specific gene associations and expression. Among several such factors that participate in the organization of a higher-order chromatin structure is the CCCTC-binding factor (CTCF), which is enriched at the boundaries of topological domains[49]. In addition, the loss of cohesin, which co-localizes with CTCF, leads to global perturbation of topological domain organization and transcriptional regulation in NPCs and NPC-derived astrocytes[51,52]. Cohesin is essential for gene expression in neural cells, and its dysfunction leads to Cornelia de Lange Syndrome (CdLS), which presents as congenital anomalies and mental retardation[53,54]. It would be interesting to map CTCF onto the genome by using chromatin immunoprecipitation in our culture system.

Several concerns regarding the 3C and its derivative techniques have been pointed out in recent publications[24,32,55]. One is that 3C ligation products largely originate from insoluble rather than soluble fractions of chromatin[56]. The results are therefore influenced by nuclear compartment or chromatin folding. Another issue is that the ability of sequences to become cross-linked and captured to distant sequences by Hi-C corresponds to the looping-out frequency from chromosome territories[57]. This indicates that the results could be affected by differences in digestion efficiency with restriction endonucleases. The modified-e4C assay with hydrochloric acid treatment used in this paper likely ameliorated this problem. Nevertheless, 3C and its derivative techniques need to be validated by completely independent methods such as FISH because the results do not always simply represent spatial proximity or molecular interaction. In addition, these methods assess millions of cells and estimate an average chromatin conformation, which prompted us to ask whether multiple identified genes simultaneously share the same nuclear locale. Three-color DNA FISH (Fig. 5C,D) showed that at least the selected three genes were rarely present in the same locale of the nucleus simultaneously. Conclusively, our results suggest that verification of results obtained with 3C and its derivatives by FISH is indispensable to give accurate insights into the nature of gene clustering. In summary, we identified genes that specifically associate with the *Gfap* gene locus and are expressed in NPC-derived astrocytes. These results suggest that transcription of one of the astrocyte-specific genes, *Gfap*, is cooperatively regulated by co-expressed genes and their regulatory factors. We provide a new framework for *Gfap* expression and astrocyte differentiation that will help uncover the precise mechanisms of *Gfap* expression and astrocyte differentiation.

Methods

Cell culture. Pregnant ICR mice were used to prepare NPCs. The experimental protocols described below were performed according to the animal experimentation guidelines of Gunma University. NPCs prepared from the telencephalon of ICR mice at embryonic day (E) 14.5 were cultured as previously described[19]. Briefly, the telencephalon was triturated in Hanks' balanced salt solution by gently pipetting with 1-mL pipette tips. Dissociated cells were cultured in N2-supplemented Dulbecco's Modified Eagle's Medium with F12 containing 10 ng/mL basic fibroblast growth factor (bFGF; R&D Systems, Minneapolis, MN) on culture dishes (Corning, Corning, NY) that were pre-coated with poly-L-ornithine and fibronectin (Sigma-Aldrich, St. Louis, MO). For astrocyte differentiation, the cells were re-plated on fibronectin/poly-L-Lysine-coated glass coverslips (MATSUNAMI, Osaka, Japan) or culture dishes that were pre-coated with poly-L-ornithine and fibronectin after 4 d of culture and were stimulated for 4 d in the presence of LIF (50 ng/mL; Millipore, Billerica, MA). All animal procedures were conducted with the approval of Gunma University Animal Care and Use Committee and were in full compliance with the Committee's guidelines.

Immunocytochemistry. Cells cultured on coated glass coverslips were fixed in 4% paraformaldehyde in phosphate-buffered saline (PBS) and washed with PBS as described previously[6]. A mouse monoclonal antibody against *GFAP* (Sigma, #G-6171) was used as a primary antibody. Alexa 555- or Alexa 647-conjugated secondary antibodies (Invitrogen, Carlsbad, CA) were used for visualization. For simultaneous labeling experiments, immunostaining was performed after FISH.

Modified e4C. e4C was performed as described previously [8] with minor modifications. Briefly, cells were exposed to 2% formaldehyde for 10 min. Cells were collected after they were quenched with 125 mM glycine. After they were homogenized, the cells were lysed in 2 mL lysis buffer (10 mM Tris-HCl [pH 7.5], 10 mM NaCl, 0.2% NP-40, 1× protease inhibitor cocktail [Nacalai Tesque]) for 1.5 h at 4 °C and centrifuged to remove the supernatant. Extracted nuclei were treated with 0.1 N HCl for 10 min and neutralized with 0.1 N NaOH and then incubated with 850 U *Bgl*II (New England Biolabs, Ipswich, MA) overnight at 37 °C. After being inactivated in 1.6% SDS at 65 °C for 20 min, samples were diluted in 4.8 mL ligation buffer (66 mM Tris-HCl [pH 7.5], 6.6 mM $MgCl_2$, 10 mM DTT, 0.1 mM ATP) and 2400 U T4 ligase (New England Biolabs) and incubated at 16 °C for 4 h. Ligated chromatin was digested by proteinase K (100 ng/mL; Merck, White House Station, NJ). After phenol-chloroform extraction, DNA was ethanol precipitated. Then, digestion efficiency was verified as previously described[58], and the 3C products were processed for primer extension with 2 U Vent (exo-) DNA polymerase (New England Biolabs) and biotinylated bait-region–specific primers. After being bound to streptavidin-coated magnetic beads (Dynabeads M-280, Invitrogen), the biotinylated products on beads were digested with 20 U *Nla*III (New England Biolabs), followed by an adaptor ligation with 2000 U T4 ligase (New England Biolabs). The beads were used for PCR with nested bait-region–specific primers and adaptor-specific primers. The amplified products were digested again with 20 U *Bgl*II and 20 U *Nla*III (New England Biolabs). Following phenol-chloroform extraction, the e4C products were ethanol precipitated. The samples were hybridized to the customized microarray following NimbleGen's protocol. The following primers

and adapters were used: 5′ GGACATGATGAGGTCCAGTC 3′ and 5′ GCTTGCTGAGGTTCTCCTAATG 3′, 5′ GCCCACGAGTGACTCACCTTG 3′ and 5′ CCAGGATGCCAGGATGTCAG 3′ (*Gfap BglII* site and GSBS for Digestion efficiency check), 5′ biotin GCTTGCTGAGGTTCTCCTAATG 3′ (biotinylated bait-specific primer for primer extension), 5′ TTGGATTTGCTGGTGCAGTACAACTAGGCTTAATAGGGACATG 3′ and 5′ phosphorylated CCCTATTAAGCCTAGTTGTACTGCACCAGCAAATCC 3′ amine C7 (Nla adapter strands), and 5′ GGATTTGCTGGTGCAGTACA 3′ and 5′ GAATAATGGCATAGTGAGGGAG 3′ (for nested PCR).

e4C microarray. e4C material was labeled and competitively hybridized with digested mouse genomic DNA as described previously [8]. The customized NimbleGen array consists of 1.4 million probes with a length of 50–70mer covering as many fragments as possible with *Bgl*II and *Nla*III sites on the 5′ and 3′ ends, respectively, and a size >100 bp based on NCBI37/mm9. Two biological replicates were performed for each condition, and reproducible positive probes were identified as e4C hits by setting a cut-off value of $\log_2$ (e4C signal/genomic control) = 2 (200-bp sliding window). e4C genes were identified by mapping all genes within 50 kb from each peak. Circos Plots of the results were generated with R version 3.3.3 using Package RCircos ver1.1.2. [59]

Sample preparation and GeneChip analysis. Sample preparation and GeneChip analysis were performed as described previously[60]. The expression data were converted to copy numbers of mRNA per cell by the Percellome method, quality controlled, and analyzed using Percellome software[25]. Genes with copy numbers that increased by at least two-fold were identified as upregulated genes, while genes whose copy numbers of mRNA were <1 were excluded.

FISH. Probes for DNA FISH were generated by nick translation of BAC clones covering genes of interest (BACPAC Resources). The following BAC clones were used: RP24–155G1 (*Gfap*), RP24–152H11 (*Ogn*), RP23–198P20 (*Osmr*), RP23–185E14 (*A2m*), RP24–214M12 (*Ecrg4*), RP24–114L21 (*Gab1*), RP23–118O2 (*Ahnak*), and RP23–211E13 (*Nme8*). FISH was essentially performed as described previously[6]. Briefly, cells were fixed with 4% PFA and kept in PBS at 4 °C until use. The cells were permeabilized with 0.5% Triton X-100/PBS and treated with 0.1 N HCl for 10 min. Cells were denatured for 30 min at room temperature in 50% formamide with 2× SSC. Hybridization was performed overnight at 37 °C with dinitrophenyl (DNP) or digoxigenin (DIG) or biotin-labeled probes and detected with Alexa 488-conjugated anti-DNP (Invitrogen) or rhodamine-conjugated anti-DIG antibody (Roche, Basel, Switzerland) or Alexa 647-conjugated streptavidin (Invitrogen). For RNA/DNA FISH, RNA probes were made as previously described[6]. In brief, *Gfap* exon sequences were amplified using cDNA prepared from astrocytes as a template. Amplified DNA was *in vitro* transcribed and then reverse-transcribed in the presence of biotin-labeled dUTP (Invitrogen). The single-stranded biotin-labeled cDNA probe was used to detect *Gfap* mRNA. Cells were fixed with 4% PFA containing 10% acetic acid and kept in 70% ethanol at −30 °C until use. Cells were digested with 0.05% pepsin/0.01 N HCl, dehydrated through ethanol treatment, and hybridized to the single-stranded DNA probe against *Gfap* cDNA. RNA-probe hybrids were detected with horseradish peroxidase-conjugated streptavidin and further labeled with Alexa598-conjugated tyramide using the TSA kit (Invitrogen). DNA FISH was performed after RNase treatment.

Microscopy and image analysis. A DeltaVision microscope (CORNES Technologies) was used to analyze the results of DNA FISH. 3D images were obtained from serial Z-sections of 8.0-μm thickness in 0.1-μm intervals. For association analysis, the shortest distances between two FISH signals were examined by softWoRx Explorer1.3 (Applied Precision). Genes were considered associated when they were positioned within 500 nm of *Gfap*.

Quantitative RT-PCR. Total RNAs were extracted with ToTALLY RNA™ Total RNA Isolation Kit and then treated with DNaseI (Life Technologies). Complementary DNAs were synthesized from 2 μg total RNA using Superscript II (Life Technologies). Quantitative real-time PCR (qPCR) was performed in an Applied Biosystems 7900HT Fast Real-Time PCR system (Life Technologies) using the KAPA SYBR Fast qPCR Kit (Kapa Biosystems, Woburn, MA). Expression of the target genes was normalized to that of glyceraldehyde-3-phosphate dehydrogenase (*Gapdh*). The following primers were used: 5′ ATCGAGATCGCCACCTACAG 3′ and 5′ CTCACATC ACCACGTCCTTG3′ (for *Gfap*), 5′ TGCAACAGGCAATTCTGAAG 3′, 5′ TGCAACAGGCAATTCTGAAG 3′ and 5′ TCCTTGGCAGTCAGCTTTTT 3′ (for *Ogn*), 5′ ACACCAAGTCCCTTCCACAG 3′ and 5′ ATGGTGACATTGG AGCCTTC 3′ (for *Osmr*), 5′ GCCTGAGGTACAGCAGTGGT 3′ and 5′ ATGGCCGCATCTTCATCATA 3′ (for *Ecrg4*), 5′ CTTCTATTATCTGATGATGGCAAAGG 3′ and 5′ CCTGCGTCACAGGCAGAAC 3′ (for *A2m*), 5′ CCAGGACG ATCCACAAGACT 3′ and 5′ TTCATTCCGTGTTTGCTCTG 3′ (for *Gab1*), 5′ ACCACAGTCCATGCCATCAC 3′ and 5′ TCCACCACCCTGTTGCTGTA 3′ (for *Gapdh*).

Statistical analyses. Residual analyses of chi-squared tests were used for Figs 4B and 5D. Fisher's and Kolmogorov-Smirnov tests were used for Fig. 5B and Figure S4, respectively. One-way analysis of variance (ANOVA) with nonparametric tests was used to compare nuclei sizes (data not shown).

Accession codes. Data are deposited in NCBI's Gene Expression Omnibus and are accessible through GEO Series accession number GSE66097.

References

1. Misteli, T. The cell biology of genomes: bringing the double helix to life. *Cell* **152,** 1209–1212 (2013).
2. Cavalli, G. & Misteli, T. Functional implications of genome topology. *Nat Struct Mol Biol* **20,** 290–299 (2013).
3. Bantignies, F. *et al.* Polycomb-dependent regulatory contacts between distant Hox loci in Drosophila. *Cell* **144,** 214–226 (2011).

4. Kohwi, M., Lupton, J. R., Lai, S. L., Miller, M. R. & Doe, C. Q. Developmentally regulated subnuclear genome reorganization restricts neural progenitor competence in Drosophila. *Cell* **152,** 97–108 (2013).
5. Osborne, C. S. *et al.* Active genes dynamically colocalize to shared sites of ongoing transcription. *Nat Genet* **36,** 1065–1071 (2004).
6. Takizawa, T., Gudla, P. R., Guo, L., Lockett, S. & Misteli, T. Allele-specific nuclear positioning of the monoallelically expressed astrocyte marker *GFAP*. *Genes Dev* **22,** 489–498 (2008).
7. Spilianakis, C. G., Lalioti, M. D., Town, T., Lee, G. R. & Flavell, R. A. Interchromosomal associations between alternatively expressed loci. *Nature* **435,** 637–645 (2005).
8. Schoenfelder, S. *et al.* Preferential associations between co-regulated genes reveal a transcriptional interactome in erythroid cells. *Nat Genet* **42,** 53–61 (2010).
9. Apostolou, E. *et al.* Genome-wide chromatin interactions of the Nanog locus in pluripotency, differentiation, and reprogramming. *Cell Stem Cell* **12,** 699–712 (2013).
10. Handoko, L. *et al.* CTCF-mediated functional chromatin interactome in pluripotent cells. *Nat Genet* **43,** 630–638 (2011).
11. Wang, K. C. *et al.* A long noncoding RNA maintains active chromatin to coordinate homeotic gene expression. *Nature* **472,** 120–124 (2011).
12. Watanabe, T. *et al.* Higher-order chromatin regulation and differential gene expression in the human tumor necrosis factor/lymphotoxin locus in hepatocellular carcinoma cells. *Mol Cell Biol* **32,** 1529–1541 (2012).
13. de Wit, E. & de Laat, W. A decade of 3C technologies: insights into nuclear organization. *Genes Dev* **26,** 11–24 (2012).
14. Li, M., Liu, G. H. & Izpisua Belmonte, J. C. Navigating the epigenetic landscape of pluripotent stem cells. *Nat Rev Mol Cell Biol* **13,** 524–535 (2012).
15. Temple, S. The development of neural stem cells. *Nature* **414,** 112–117, doi: 10.1038/35102174 (2001).
16. Edlund, T. & Jessell, T. M. Progression from extrinsic to intrinsic signaling in cell fate specification: a view from the nervous system. *Cell* **96,** 211–224 (1999).
17. Hsieh, J. & Gage, F. H. Epigenetic control of neural stem cell fate. *Curr Opin Genet Dev* **14,** 461–469 (2004).
18. Hatada, I. *et al.* Astrocyte-specific genes are generally demethylated in neural precursor cells prior to astrocytic differentiation. *PLoS One* **3,** e3189 (2008).
19. Takizawa, T. *et al.* DNA methylation is a critical cell-intrinsic determinant of astrocyte differentiation in the fetal brain. *Dev Cell* **1,** 749–758 (2001).
20. Nakashima, K. *et al.* Synergistic signaling in fetal brain by STAT3-Smad1 complex bridged by p300. *Science* **284,** 479–482 (1999).
21. Nakashima, K. *et al.* Developmental requirement of gp130 signaling in neuronal survival and astrocyte differentiation. *J Neurosci* **19,** 5429–5434 (1999).
22. Urayama, S. *et al.* Chromatin accessibility at a STAT3 target site is altered prior to astrocyte differentiation. *Cell Struct Funct* **38,** 55–66 (2013).
23. Peric-Hupkes, D. *et al.* Molecular maps of the reorganization of genome-nuclear lamina interactions during differentiation. *Mol Cell* **38,** 603–613 (2010).
24. Belmont, A. S. Large-scale chromatin organization: the good, the surprising, and the still perplexing. *Curr Opin Cell Biol* **26,** 69–78 (2014).
25. Kanno, J. *et al.* "Per cell" normalization method for mRNA measurement by quantitative PCR and microarrays. *BMC Genomics* **7,** 64 (2006).
26. Duchemin, A. M., Ren, Q., Neff, N. H. & Hadjiconstantinou, M. GM1-induced activation of phosphatidylinositol 3-kinase: involvement of Trk receptors. *J Neurochem* **104,** 1466–1477 (2008).
27. Gonzalez, A. M. *et al.* Ecrg4 expression and its product augurin in the choroid plexus: impact on fetal brain development, cerebrospinal fluid homeostasis and neuroprogenitor cell response to CNS injury. *Fluids Barriers CNS* **8,** 6 (2011).
28. Jeong, E. Y. *et al.* Enhancement of IGF-2-induced neurite outgrowth by IGF-binding protein-2 and osteoglycin in SH-SY5Y human neuroblastoma cells. *Neurosci Lett* **548,** 249–254 (2013).
29. Kovacs, D. M. alpha2-macroglobulin in late-onset Alzheimer's disease. *Exp Gerontol* **35,** 473–479 (2000).
30. Van Wagoner, N. J., Choi, C., Repovic, P. & Benveniste, E. N. Oncostatin M regulation of interleukin-6 expression in astrocytes: biphasic regulation involving the mitogen-activated protein kinases ERK1/2 and p38. *J Neurochem* **75,** 563–575 (2000).
31. Simonis, M., Kooren, J. & de Laat, W. An evaluation of 3C-based methods to capture DNA interactions. *Nat Methods* **4,** 895–901 (2007).
32. Williamson, I. *et al.* Spatial genome organization: contrasting views from chromosome conformation capture and fluorescence *in situ* hybridization. *Genes Dev* **28,** 2778–2791 (2014).
33. Namihira, M., Nakashima, K. & Taga, T. Developmental stage dependent regulation of DNA methylation and chromatin modification in a immature astrocyte specific gene promoter. *FEBS Lett* **572,** 184–188 (2004).
34. Chen, X. *et al.* Integration of external signaling pathways with the core transcriptional network in embryonic stem cells. *Cell* **133,** 1106–1117 (2008).
35. Cook, P. R. The organization of replication and transcription. *Science* **284,** 1790–1795 (1999).
36. Li, G. *et al.* Extensive promoter-centered chromatin interactions provide a topological basis for transcription regulation. *Cell* **148,** 84–98 (2012).
37. Yanagisawa, M., Nakashima, K. & Taga, T. STAT3-mediated astrocyte differentiation from mouse fetal neuroepithelial cells by mouse oncostatin M. *Neurosci Lett* **269,** 169–172 (1999).
38. Clarkson, R. W. *et al.* The genes induced by signal transducer and activators of transcription (STAT)3 and STAT5 in mammary epithelial cells define the roles of these STATs in mammary development. *Mol Endocrinol* **20,** 675–685 (2006).
39. Tiffen, P. G. *et al.* A dual role for oncostatin M signaling in the differentiation and death of mammary epithelial cells *in vivo*. *Mol Endocrinol* **22,** 2677–2688 (2008).
40. Kujuro, Y., Suzuki, N. & Kondo, T. Esophageal cancer-related gene 4 is a secreted inducer of cell senescence expressed by aged CNS precursor cells. *Proc Natl Acad Sci USA* **107,** 8259–8264 (2010).
41. Le May, N., Fradin, D., Iltis, I., Bougneres, P. & Egly, J. M. XPG and XPF endonucleases trigger chromatin looping and DNA demethylation for accurate expression of activated genes. *Mol Cell* **47,** 622–632 (2012).
42. Ling, J. Q. *et al.* CTCF mediates interchromosomal colocalization between Igf2/H19 and Wsb1/Nf1. *Science* **312,** 269–272 (2006).
43. Takebayashi, S., Dileep, V., Ryba, T., Dennis, J. H. & Gilbert, D. M. Chromatin-interaction compartment switch at developmentally regulated chromosomal domains reveals an unusual principle of chromatin folding. *Proc Natl Acad Sci USA* **109,** 12574–12579 (2012).
44. Cheng, P. Y. *et al.* Interplay between SIN3A and STAT3 mediates chromatin conformational changes and *GFAP* expression during cellular differentiation. *PLoS One* **6,** e22018 (2011).
45. Song, M. R. & Ghosh, A. FGF2-induced chromatin remodeling regulates CNTF-mediated gene expression and astrocyte differentiation. *Nat Neurosci* **7,** 229–235 (2004).
46. Tan, S. L. *et al.* Essential roles of the histone methyltransferase ESET in the epigenetic control of neural progenitor cells during development. *Development* **139,** 3806–3816 (2012).
47. Tiwari, V. K. *et al.* PcG proteins, DNA methylation, and gene repression by chromatin looping. *PLoS Biol* **6,** 2911–2927 (2008).
48. Sparmann, A. *et al.* The chromodomain helicase Chd4 is required for Polycomb-mediated inhibition of astroglial differentiation. *Embo J* **32,** 1598–1612 (2013).

49. Dixon, J. R. *et al.* Topological domains in mammalian genomes identified by analysis of chromatin interactions. *Nature* **485,** 376–380 (2012).
50. Holwerda, S. & de Laat, W. Chromatin loops, gene positioning, and gene expression. *Front Genet* **3,** 217 (2012).
51. Wendt, K. S. *et al.* Cohesin mediates transcriptional insulation by CCCTC-binding factor. *Nature* **451,** 796–801 (2008).
52. Sofueva, S. *et al.* Cohesin-mediated interactions organize chromosomal domain architecture. *Embo J* **32,** 3119–3129 (2013).
53. Liu, J. & Baynam, G. Cornelia de Lange syndrome. *Adv Exp Med Biol* **685,** 111–123 (2010).
54. Chang, J. *et al.* Nicotinamide adenine dinucleotide (NAD)-regulated DNA methylation alters CCCTC-binding factor (CTCF)/cohesin binding and transcription at the BDNF locus. *Proc Natl Acad Sci USA* **107,** 21836–21841 (2010).
55. Pombo, A. & Dillon, N. Three-dimensional genome architecture: players and mechanisms. *Nat Rev Mol Cell Biol* **16,** 245–257 (2015).
56. Gavrilov, A. A. *et al.* Disclosure of a structural milieu for the proximity ligation reveals the elusive nature of an active chromatin hub. *Nucleic Acids Res* **41,** 3563–3575 (2013).
57. Kalhor, R., Tjong, H., Jayathilaka, N., Alber, F. & Chen, L. Genome architectures revealed by tethered chromosome conformation capture and population-based modeling. *Nat Biotechnol* **30,** 90–98 (2012).
58. Hagege, H. *et al.* Quantitative analysis of chromosome conformation capture assays (3C-qPCR). *Nat Protoc* **2,** 1722–1733 (2007).
59. Zhang, H., Meltzer, P. & Davis, S. RCircos: an R package for Circos 2D track plots. *BMC Bioinformatics* **14,** 244 (2013).
60. Sanosaka, T. *et al.* Identification of genes that restrict astrocyte differentiation of midgestational neural precursor cells. *Neuroscience* **155,** 780–788, 2008.06.039 (2008).

Acknowledgements

We thank all members of department of Pediatrics for their help and advice. We thank P. Fraser for kindly providing the e4C protocol. We also thank M. Nakao, N. Saito, T. Watanabe, and S. Tomita for valuable discussion and technical advice. This work was supported by a Grant-in-Aid for Scientific Research on Innovative Areas 23114714 and a grant from the JST Strategic International Research Cooperative Program, SICP.

Author Contributions

T.T. designed the experiments. K.I.[1], T.S., K.I.[3] and M.O. performed the experiments. K.I.[1], T.S. and A.A. analyzed the data. K.I.[1] and T.T. wrote the manuscript. K.N., A.N., Y.U. and H.A. participated in discussions and gave valuable suggestions. All authors reviewed the paper.

Additional Information

Supplementary information accompanies this paper at http://www.nature.com/srep

Competing financial interests: The authors declare no competing financial interests.

How to cite this article: Ito, K. *et al.* Identification of genes associated with the astrocyte-specific gene *Gfap* during astrocyte differentiation. *Sci. Rep.* **6,** 23903; doi: 10.1038/srep23903 (2016).

Neuroepigenetics 5 (2016) 1–10

Contents lists available at ScienceDirect

Neuroepigenetics

journal homepage: WWW.ELSEVIER.COM/LOCATE/NEPIG

Epigenetic regulation of neural stem cell property from embryo to adult

Naoya Murao [1], Hirofumi Noguchi [1], Kinichi Nakashima *

Stem Cell Biology and Medicine, Department of Stem Cell Biology and Medicine, Graduate School of Medical Sciences, Kyushu University, Fukuoka, Japan

ARTICLE INFO

Article history:
Received 2 September 2015
Received in revised form 8 January 2016
Accepted 8 January 2016
Available online xxxx

ABSTRACT

Neural stem cells (NSCs) have the ability to self-renew and give rise to neurons and glial cells (astrocytes and oligodendrocytes) in the mammalian central nervous system. This multipotency is acquired by NSCs during development and is maintained throughout life. Proliferation, fate specification, and maturation of NSCs are regulated by both cell intrinsic and extrinsic factors. Epigenetic modification is a representative intrinsic factor, being involved in many biological aspects of central nervous system development and adult neurogenesis through the regulation of NSC dynamics. In this review, we summarize recent progress in the epigenetic regulation of NSC behavior in the embryonic and adult brain, with particular reference to DNA methylation, histone modification, and noncoding RNAs.

1. Introduction

Neural stem cells (NSCs) are defined as cells that have the capacity for self-renewal and differentiation into 3 cell types: neurons and 2 types of glial cells, astrocytes, and oligodendrocytes. Neurogenesis, the process by which neurons are generated from NSCs, occurs not only in the embryonic but also in the postnatal/adult brain. Neurogenesis takes place in particular zones throughout organism's lifespan and has been implicated in various brain functions, such as learning and memory (Bond et al., 2015; Christian et al., 2014; Gotz and Huttner, 2005; Greig et al., 2013; Hsieh and Eisch, 2010; Kriegstein and Alvarez-Buylla, 2009; Lledo et al., 2006; Miller and Gauthier, 2007; Ming and Song, 2011). Therefore, neurogenesis is an important process for both brain development and brain function.

During embryonic brain development, NSCs show unique features as they produce each type of cell in the brain. The onset of neurogenesis and gliogenesis is spatiotemporally restricted in the developing brain, in which NSCs generate each type of cell in a developmental stage-dependent manner: neurons are produced first, followed by glial cells. This change in the differentiation capacity of NSCs as development proceeds is tightly regulated through cooperation between extracellular factors and epigenetic mechanisms. In addition, NSCs that have been maintained until adulthood mainly produce neurons, and this adult neurogenesis consists of multiple steps. NSCs generate neurons via the production of transiently amplifying neuronal precursor cells (NPCs) through asymmetrical division. Thus, adult neurogenesis starts from the activation of NSC proliferation, which is followed by production of NPCs and their differentiation into neurons. Moreover, newly generated neurons are integrated into preexisting neuronal circuitry, thereby contributing to brain functions. Survival and maturation of newborn neurons are thus also key steps for adult neurogenesis to occur properly. In addition to embryonic neurogenesis, accumulating research in adult neurogenesis has been highlighting the importance of epigenetic regulation to control these processes.

Epigenetics can be defined as heritable influences on chromatin and gene function that are not accompanied by a change in DNA sequence in the progeny of cells or individuals (Allis et al., 2015). DNA methylation, histone modification, and noncoding RNAs are predominant epigenetic factors and have been studied for the last 2 decades. These studies have demonstrated that distinct epigenetic factors communicate with each other and play an essential role for the regulation of NSCs in collaboration with extracellular cues. In this review, we introduce representative examples of epigenetic mechanisms involved in the dynamics of embryonic and adult NSCs.

1.1. Epigenetic mechanisms regulating neurogenic and gliogenic competence of NSCs during development

Although the 3 types of cells in the brain are generated from NSCs during central nervous system (CNS) development, NSCs do not initially have the potential to generate these cell types. NSCs acquire this competence sequentially as development proceeds. After NSCs expand their pool by self-renewing in early brain development, they first produce neurons, followed by astrocytes and oligodendrocytes (Fig. 1). Many factors that induce NSC differentiation into each lineage have been identified, including Wingless/int (Wnt, neurons) (Hirabayashi et al., 2004; Muroyama et al., 2004; Zhou et al.,

* Corresponding author.
E-mail address: kin1@scb.med.kyushu-u.ac.jp (K. Nakashima).
[1] These authors contributed equally.

http://dx.doi.org/10.1016/j.nepig.2016.01.001

2006a), leukemia inhibitory factor (astrocytes) (Bugga et al., 1998; Nakashima et al., 1999a,b; Namihira and Nakashima, 2013), and Sonic hedgehog (Shh, oligodendrocytes) (Lu et al., 2000; Tekki-Kessaris et al., 2001). Recent studies have indicated that the way in which NSCs respond to these factors alters during development and that epigenetic mechanisms restrict the responsiveness of NSCs to them at each stage of development. This contributes to the sequential production of neurons and glial cells during development. In this section, we describe how NSCs sequentially acquire the competence to generate cells in each lineage during development, focusing on the epigenetic mechanisms in the order of histone modification, DNA methylation, and noncoding RNAs.

1.2. Histone modification regulating differentiation of NSCs

The remodeling of chromatin structure via histone modifications is an important means of modulating gene expression. Chromatin is composed of multiple nucleosomes, each consisting of 147 base pairs of DNA wrapped around histone proteins. Single nucleosomes contain 2 copies of each histone variant: histone 2A, histone 2B, histone 3 (H3), and histone 4. The amino acid residues in the N-terminal tails of histone proteins are subject to multiple posttranscriptional modifications, including acetylation, methylation, phosphorylation, and ubiquitination (Bernstein et al., 2007; Kouzarides, 2007; Margueron and Reinberg, 2010; Ruthenburg et al., 2007; Tessarz and Kouzarides, 2014). Histone modifications affect the access of transcription factors to their binding sites, thereby influencing gene activation and repression. For instance, lysine methylation of histone tails is associated with both activation and repression of gene expression; the effect of histone methylation on gene expression differs according to the position in the histone tail and the number of methylation in the lysine residues. H3 methylation at lysine 4 (K4), K36, and K79 leads to transcriptional activation, whereas H3 methylation at K9 and K27 is associated with transcriptional silencing. Both neurogenic and gliogenic gene promoters undergo various histone modifications, which ensure the sequential production of each cell type at appropriate stages of development.

Neuronal differentiation precedes glial differentiation of NSCs during development, and NSCs terminate neuronal production gradually as glial differentiation commences. The reduction of neuronal differentiation results from a change in the responsiveness of NSCs to Wnt/β-catenin signaling. Activation of Wnt/β-catenin signaling induces neuronal differentiation during midgestation (neurogenic phase) through up-regulation of the proneural basic helix-loop-helix (bHLH) transcription factor neurogenin1 (Neurog1) (Hirabayashi et al., 2004; Sun et al., 2001). However, *Neurog1* expression is no longer induced in NSCs at late gestation, when astrogliogenesis from NSCs begins, even when Wnt/β-catenin signaling is activated. This different responsiveness of NSCs to Wnt/β-catenin signaling at each developmental stage is attributed to a change in histone modification status on the *Neurog1* promoter.

The polycomb group (PcG) complex catalyzes H3 K27 trimethylation (H3K27me3), leading to transient transcriptional repression through alteration of local heterochromatin configuration (Ng and Gurdon, 2008; Ringrose and Paro, 2007). The PcG consists of 2 complexes, polycomb repressive complex 1 (PRC1) and polycomb repressive complex 2 (PRC2). PRC2 is responsible for the initiation of gene silencing by catalyzing H3K27me3, which provides a mark for PRC1 to be recruited for gene silencing. PRC1 maintains H3K27me3 and takes part in compacting chromatin states (Cao and Zhang, 2004; Shen et al., 2008).

One of the PRC2 components, enhancer of zeste 2 (Ezh2), an enzyme responsible for H3K27me3, is highly expressed in NSCs in the gliogenic phase and prevents Wnt signaling–mediated expression of

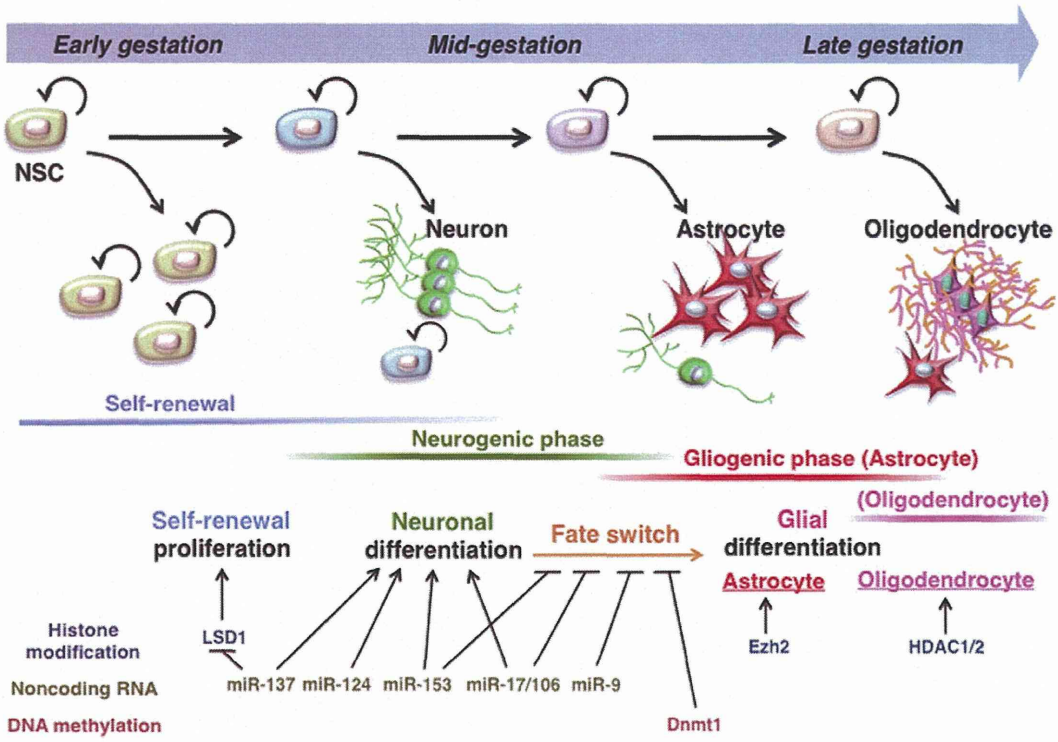

Fig. 1. Schematic diagram of developmental stage-dependent NSC differentiation in the embryonic brain. During early embryonic stages, NSCs undergo self-renewing symmetric divisions, leading to the expansion of their pool. NSCs first acquire the potential to differentiate into neurons at midgestation. They then acquire the ability to differentiate into glial cells from late to perinatal stages. Representative epigenetic regulators of NSCs during embryonic brain development are depicted. Semicircular arrows indicate the self-renewal and proliferation of NSCs. →, promotion; ⊣, inhibition.

neuronal genes at the onset of astrogliogenesis (Hirabayashi et al., 2009; Pereira et al., 2010) (Fig. 1). Consistent with the loss of neurogenic competence of NSCs during development, *Neurog1* gains H3K27me3 in the promoter, and its expression becomes repressed as NSC differentiation leans toward astrocyte production. Ezh2 directly targets *Neurog1* and suppresses its expression by catalyzing H3K27me3 in the promoter region (Hirabayashi et al., 2009). This eventually limits the responsiveness of NSCs to Wnt signaling and contributes to switching the competence of NSCs from neurogenic to gliogenic. In fact, NSC-specific conditional deletion of *Ezh2* before the onset of astrocyte differentiation prolongs neuronal production and delays the production of astrocytes (Pereira et al., 2010).

Polycomb repressive complexes also affect layer formation of the cortex. Newly generated neurons migrate to the outside of the cortical plate along with radial processes of NSCs, which extend to the pial surface, and establish the cortical layer in an inside-out order: deep layer (DL) neurons are generated first, followed by upper layer (UL) neurons (Greig et al., 2013; Molyneaux et al., 2007). The Fez transcription factor family member zinc-finger 2 (Fezf2) plays a key role in the differentiation of NSCs into DL neurons, and its expression governs the period for the production of DL neurons (Chen et al., 2005a, 2005b; Molyneaux et al., 2005). Ring1B, one of the components of PRC1, represses the expression of Fezf2 and contributes to the termination of DL neuron production. Deletion of *Ring1B* in NSCs prolongs the expression of Fezf2, resulting in increased production of DL neurons (Morimoto-Suzki et al., 2014).

Histone acetylation also affects appropriate layer formation by regulating the fate propensity of NSCs from DL neurons to UL neuron production. Acetylation of histone N-terminal tails induces relaxation of the nucleosomes by decreasing the interaction of the positively charged histone tails with the negatively charged DNA. Histone deacetylases (HDACs) condense chromatin by removing acetyl groups from histone tails, which prevents the access of transcription factors to their cognate sites and leads to transcriptional repression. Blocking HDAC activity in the neurogenic phase, using the HDAC inhibitor suberoylanilide hydroxamic acid, decreases the production of DL neurons and increased UL neurons from NSCs (Yuniarti et al., 2013). This finding suggests that histone acetylation participates in the transition from DL neuron to UL neuron production during cortical development.

As in neuronal differentiation, bHLH transcriptional factors play a critical role in oligodendrocyte differentiation. Shh signaling is highly activated in the ganglionic eminence of the ventral telencephalon, where oligodendrocytes are induced by the Shh-induced bHLH transcriptional factors Olig1 and Olig2 (Lu et al., 2000; Tekki-Kessaris et al., 2001). These 2 factors play essential roles in oligodendrocyte differentiation and maturation. Compound *Olig1* and *Olig2* knock-out (KO) mice displayed complete loss of oligodendrocytes (Zhou and Anderson, 2002). Olig2 is essential for the initiation of oligodendrocyte differentiation, whereas Olig1 is required for the maturation of oligodendrocytes and the remyelination of axons after oligodendrocyte ablation (Arnett et al., 2004; Dai et al., 2015; Liu et al., 2007; Xin et al., 2005). bHLH transcription factors activate expression of downstream targets by forming dimers with ubiquitously expressed bHLH E-proteins such as E12 and E47. However, the negative HLH factors hairy and enhancer of split (Hes) and inhibitor of differentiation (Id) inhibit bHLH transcription factors by competing with them for dimerization with E-proteins. Wnt signal activation induces expression of the negative HLH factors Id2 and 4, limiting the generation of oligodendrocytes (Ye et al., 2009). The activation of Wnt signaling declines at the onset of oligodendrocyte differentiation, implying that Wnt signaling influences the timing of oligodendrocyte differentiation during brain development (Langseth et al., 2010).

HDACs modulate the inhibition of oligodendrocyte production by Wnt signaling and ensure oligodendrocyte development. HDAC activity is essential for the development and maturation of oligodendrocytes: treatment with HDAC inhibitor attenuates oligodendrocyte differentiation (Marin-Husstege et al., 2002), and HDAC1 and HDAC2 double KO mice show severe defects in oligodendrocyte production and maturation (Ye et al., 2009) (Fig. 1). Wnt signaling stabilizes β-catenin, which then induces downstream targets of Wnt signaling, such as Id2 and 4, by forming a complex with transcription factor 7–like 2 (TCF7L2), a downstream effector. HDAC1 and 2 bind competitively to TCF7L2 with β-catenin, thereby inhibiting expression of the *Id2* and *4* genes (Ye et al., 2009). Another HDAC partner that promotes differentiation of oligodendrocytes, Yin Yang 1 (YY1), has been identified through a binding motif analysis in the promoters of up-regulated genes involving treatment with HDAC inhibitor. The *Id4* and *TCF7L2* promoters contain a YY1 binding site, and YY1 inhibits expression of these genes by recruiting HDAC1 and 2 to their promoters (He et al., 2007) (Fig. 1).

1.3. Role of DNA methylation in regulating gliogenic competence of NSCs

After the production of neurons, NSCs start to give rise to astrocytes. The later onset of astrogliogenesis results from a dramatic change of DNA methylation in astrocyte-specific promoters. DNA methylation predominantly occurs at the cytosine residue of CpG dinucleotides in the mammalian genome. DNA methylation in gene promoters has been associated with gene repression and stem cell differentiation in various tissues, including the CNS. *Glial fibrillary acidic protein* (*Gfap*) and *S100β* are representative genes that are expressed specifically in astrocytes. Their promoters are highly methylated in NSCs from early to midgestational stages, limiting the responsiveness of NSCs to astrocyte differentiation–inducing factors. Members of the interleukin 6 family of cytokines, such as leukemia inhibitory factor and ciliary neurotrophic factor, have been identified as astrocyte-inducing factors. These factors induce astrocyte differentiation of NSCs by activating the Janus kinase (JAK) signal transducer and activator of transcription 3 (STAT3) pathway. Astrocyte-specific genes, including *Gfap* and *S100β*, have STAT-binding sites in their promoters, and their expression is induced by activation of the JAK-STAT pathway during the gliogenic phase. However, NSCs in the neurogenic phase fail to express these genes even if the JAK-STAT pathway is activated. This is because STAT3-binding sites are methylated in NSCs, which interferes with the binding of STAT3 to the promoter region, resulting in the inhibition of astrocyte-specific gene expression during the neurogenic phase (Bonni et al., 1997; He et al., 2005; Nakashima et al., 1999a,b; Namihira and Nakashima, 2013; Rajan and McKay, 1998). Methylated DNA in astrocyte-specific genes undergoes demethylation during development, enabling NSCs to respond to astrocyte-inducing factors. Thus, demethylation of astrocyte-specific gene promoters explains, at least partially, how NSCs switch their competence from neurogenic to gliogenic. In support of this model, deletion of the gene encoding DNA methyltransferase 1 (Dnmt1), an enzyme responsible for the maintenance of DNA methylation after DNA replication, causes precocious astrocyte differentiation of NSCs in the neurogenic phase (Fan et al., 2005) (Fig. 1).

These findings raise further question of how DNA demethylation of astrocyte-specific genes occurs. Demethylation of DNA occurs via 2 distinct processes. One of these is passive demethylation, which progresses in a DNA replication–dependent manner as Dnmt1 is excluded from the methylation target site. Because neurons are the first cell type produced by NSCs during development—meaning that neurons are the first cell type with which NSCs make contact, other than NSCs themselves—we hypothesized that some signal from neurons triggers DNA demethylation and confers the competence to produce astrocytes on remaining NSCs. Newly generated immature neurons express the ligands of Notch, Delta-like 1 and JAGGED1, and they activate Notch signaling, which induces expression of nuclear factor IA (NFIA) in remaining NSCs (Namihira et al., 2009; Namihira and Nakashima, 2013). NFIA then binds to the astrocyte-specific gene promoters, which leads to the dissociation of Dnmt1 from the

promoters, thus preventing Dnmt1 from maintaining DNA methylation. This partially accounts for how DNA demethylation of astrocyte-specific gene promoters is induced during development and also why astrocyte production begins following the neurogenic phase. However, the precise molecular mechanism of how binding of NFIA leads to the dissociation of Dnmt1 from astrocyte-specific gene promoters remains elusive. It has been shown that, during DNA replication, Dnmt1 is recruited to methylation target sites by Uhrf1 (ubiquitin-like containing PHD and RING finger domains 1; also known as Np95), which is highly expressed by NSCs in the developing brain (Bostick et al., 2007; Murao et al., 2015; Sharif et al., 2007). Therefore, Uhrf1 may be involved in the mechanism by which NFIA induces exclusion of Dnmt1 from the target site. In any case, a more detailed mechanism to explain DNA demethylation in astrocyte-specific genes must await further investigation.

Another mechanism for DNA demethylation is active demethylation, which occurs in a replication-independent manner, and this is mediated by Ten-eleven translocation (TET) family proteins. TETs convert 5′-methylcytosine (5mC) to 5′-hydroxymethylcytosine (5hmC) in a Fe (II)– and α-ketoglutarate–dependent fashion (Pastor et al., 2013; Wu and Zhang, 2010). 5hmC is thought to serve as an intermediate in the active DNA demethylation process (Kohli and Zhang, 2013). TET proteins further oxidize 5hmC to 5-formylcytosine (5fC) and 5-carboxylcytosine (5caC). These oxidized cytosines can then be successively excised by thymine-DNA glycosylase (TDG) followed by replacement with unmodified 5mC via the base excision repair pathway (He et al., 2011; Ito et al., 2011; Kohli and Zhang, 2013; Zhang et al., 2012).

During embryonic brain development, high levels of 5hmC are detected in the cortical plate, and the levels increase with neuronal differentiation (Hahn et al., 2013). This enrichment of 5hmC inversely correlates with H3K27me3. 5hmC is observed in the gene body of neuronal function–related genes, such as *sex-determining region Y (SRY)-related HMG box 5* (*Sox5*), *B-cell chronic lymphocytic leukemia/lymphoma 11B* (*Bcl11b*), and *myelin transcription factor 1-like* (*Myt1l*). Concomitant with their expression, these genes lose H3K27me3 from their promoter and gain 5hmC marks in the gene body during the progression of neuronal differentiation. This unique mode of occupancy of 5hmC and H3K27me3 is indicative of its mechanistic role in neuronal differentiation of NSCs. In fact, knockdown (KD) of Ezh2 promotes the neuronal differentiation of NSCs, and overexpression of Tet1 and Tet2 further enhances the Ezh2 KD-promoted neuronal differentiation. This suggests that formation of 5hmC and loss of H3K27me3 cooperate to promote neuronal differentiation during the neurogenic phase (Hahn et al., 2013). Interestingly, enrichment of 5hmC during this time does not lead to substantial DNA demethylation, suggesting that 5hmC functions as a stable epigenetic mark and takes part in regulating gene expression.

Similar to the enrichment of 5hmC, 5caC also displays transient accumulation in the genome specifically during differentiation of NSCs (Wheldon et al., 2014), and the accumulation of 5caC becomes more obvious as NSCs are stimulated to differentiate into glial cells. Indeed, TDG KD increased 5caC and 5fC levels during glial differentiation. In particular, glial gene promoters such as *Gfap*, *Olig1*, and *Olig2* acquire 5caC and 5fC during glial differentiation. Given that TDG excises both 5caC and 5fC and leads to DNA demethylation, this enrichment of 5caC in the promoters of astrocyte-specific genes such as *Gfap* suggests the possibility that DNA demethylation of astrocyte-specific genes also occurs through active DNA demethylation. Whatever the mechanism, these findings support the idea that DNA demethylation warrants the timing of gliogenesis in the developing brain.

1.4. Role of noncoding RNAs in embryonic NSC differentiation

Noncoding RNAs are transcribed from DNA but not translated into proteins. Among these, microRNAs (miRNAs) and long noncoding RNA (lncRNA) play a variety of roles in fine-tuning gene expression by transcriptional and posttranscriptional regulation. miRNAs are known to contribute to posttranscriptional repression of gene expression and have been explored extensively in recent years. These studies have shown that, in addition to histone modification and DNA methylation, noncoding RNAs also participate in the mechanisms that ensure the sequential production of distinct neural cell types from NSCs during development.

Chicken ovalbumin upstream promoter-transcription factor I and II (COUP-TFI/II) induces competence transition of NSCs from neurogenic to gliogenic during development. The expression of COUP-TFI/II is high in the gliogenic phase, and this facilitates the DNA demethylation of the *Gfap* promoter (Naka et al., 2008). A recent study has identified miR-17/106, whose expression in NSCs increases in the neurogenic phase and gradually decreases along with the transition to the gliogenic phase, as a downstream effector of COUP-TFI/II (Naka-Kaneda et al., 2014). miR-17/106 targets p38 (also known as MAPK14) to regulate the transition of NSC competence and plays an essential role in determining the responsiveness of NSCs to gliogenic signals (Fig. 1). Overexpression of p38 or suppression of miR-17/106 in embryonic stem cell–derived neurogenic NSCs induces precocious astrocytic differentiation in the presence of astrocyte differentiation-inducing factors. Therefore, the COUP-TFI/II–miR-17/106–p38 axis is a critical regulator for the neurogenic-to-gliogenic NSC competence transition.

Moreover, miR-153 also regulates the acquisition of gliogenic potential of NSCs (Tsuyama et al., 2015) (Fig. 1). miR-153 targets messenger RNAs (mRNAs) for NFIA and B, 2 essential regulators for the initiation of gliogenesis that act by inducing demethylation of astrocytic gene promoters. Gain- and loss-of-function experiments using miR-153 in vitro and in vivo suggest that miR-153–mediated fine tuning of NFIA and B expression is essential for the acquisition of gliogenic potential by NSCs during CNS development.

In addition to these miRNAs, a very recent study has revealed that miR-9, which shows specific enrichment in the brain, is also involved in fate specification of NSCs (Zhao et al., 2015) (Fig. 1). miR-9 is induced by Neurog1, and it directly targets mRNA of *Lif receptor beta* (*Lifr-beta*), *Il-6 signal transducer* (*Il6st*), and *Jak1*, which are major components of the JAK-STAT pathway, resulting in the inhibition of astrogliogenesis during the neurogenic stage. miR-9 KD in neurogenic NSCs increased astrocyte differentiation both in vitro and in vivo, whereas its overexpression decreased it. Therefore, as well as miR-17/106 and miR-153, miR-9 is also an important regulator for the fate specification of NSCs.

Furthermore, many other miRNAs have been identified as being specifically expressed in the mammalian brain. For example, Let-7 and miR-137 are highly expressed from the embryonic to the adult brain. In addition, each neural cell type differentially expresses distinct miRNAs: miR-124 is highly expressed in neurons, whereas miR-23, 26, 29, and 146a are predominantly expressed in astrocytes (Iyer et al., 2012; Smirnova et al., 2005). These cell type–specific expression patterns of miRNAs suggest their critical roles in regulating some function in each cell type, such as NSC proliferation and differentiation.

Among these miRNAs, miR-124 comprises 25%–48% of total miRNAs in the brain and has been extensively studied (Lagos-Quintana et al., 2002). miR-124, whose expression increases during brain development, promotes neuronal differentiation of NSCs (Fig. 1). miR-124 directly targets the small C-terminal domain phosphatase 1 (SCP1), an antineural factor expressed in nonneuronal tissues. SCP1 is recruited to repressor element 1–containing neural genes by repressor element 1 silencing transcription factor (REST), also known as neuron-restrictive silencer factor, and is involved in their repression (Visvanathan et al., 2007; Yeo et al., 2005). miR-124 suppresses SCP1 expression during CNS development, thereby inducing neurogenesis. In addition, miR-124 down-regulates the expression of the RNA-binding protein polypyrimidine tract binding protein 1, a global repressor of CNS-specific alternative pre-mRNA